PNAS RESEARCH ARTICLE | EVOLUTION

The sea spider *Pycnogonum litorale* overturns the paradigm of the absence of axial regeneration in molting animals

Georg Brenneis[a,b,1], Karina Frankowski[a], Laura Maaß[a], and Gerhard Scholtz[c]

Edited by Lynn Riddiford, University of Washington, Friday Harbor, WA; received October 9, 2022; accepted December 9, 2022

Regenerative abilities and their evolution in the different animal lineages have fascinated generations of biologists. While some taxa are capable of restoring entire individuals from small body fragments, others can regrow only specific structures or lack structural regeneration completely. In contrast to many other protostomes, including the segmented annelids, molting animals (Ecdysozoa) are commonly considered incapable of primary body axis regeneration, which has been hypothesized to be linked to the evolution of their protective cuticular exoskeleton. This holds also for the extraordinarily diverse, segmented arthropods. Contradicting this long-standing paradigm, we here show that immatures of the sea spider *Pycnogonum litorale* reestablish the posterior body pole after transverse amputation and can regrow almost complete segments and the terminal body region, including the hindgut, anus, and musculature. Depending on the amputation level, normal phenotypes or hypomeric six-legged forms develop. Remarkably, also the hypomeric animals regain reproductive functionality by ectopic formation of gonoducts and gonopores. The discovery of such complex regenerative patterns in an extant arthropod challenges the hitherto widely assumed evolutionary loss of axial regeneration during ecdysozoan evolution. Rather, the branching of sea spiders at the base of Chelicerata and their likely ancestral anamorphic development suggests that the arthropod stem species may have featured similar regenerative capabilities. Accordingly, our results provide an incentive for renewed comparative regeneration studies across ecdysozoans, with the aim to resolve whether this trait was potentially even inherited from the protostome ancestor.

Arthropoda | Pycnogonida | evolution | segmentation | development

Significance

Unlike many other animals, the molting ecdysozoans are thought to lack the potential of main body axis regeneration after traumatic injury. This includes today's most diverse lineage—the segmented Arthropoda—implying that axial regenerative capabilities did not contribute to its extraordinarily successful evolutionary radiation. Challenging these long-held views, we show that sea spiders can regrow a functional hindbody region after experimental removal, including the restoration of the reproductive system. Given the branching of sea spiders near the base of the arthropod tree, this leads us to suggest that the arthropod stem species may have been capable of posterior axial regeneration. Pending additional studies on nonarthropod ecdysozoans, this may even represent a trait inherited from the protostome ancestor.

The study of animal regeneration and its evolution has a long history and continues to be a vibrant research field (1–4), not least since a detailed understanding of the developmental mechanisms governing the restoration of damaged tissues and lost body parts holds great promise for regenerative medicine. Notably, the regenerative potential varies considerably between animal taxa and is unevenly spread across the animal tree of life (2, 5, 6). While representatives of some groups (e.g., cnidarians, flatworms, echinoderms) may regenerate entire individuals from tiny body pieces, others can restore only certain structures (such as legs or tails) or are incapable of any structural regeneration (7).

The segmented arthropods (chelicerates, myriapods, crustaceans, and hexapods) represent today's most diverse animal lineage that inhabits virtually all aquatic habitats and has successfully conquered land and air in the course of its impressive evolutionary radiation (8). Regeneration of appendages is well-documented for various arthropod lineages (2, 5, 9, 10) and may in some taxa even follow self-amputation of limbs at predefined breaking points (autotomy) to escape predation or during molting complications (11). By contrast, the ability to restore lost elements of the primary body axis (anterior and posterior body regions and body segments) is commonly acknowledged to be lacking (5, 12). Like all molting animals (Ecdysozoa), arthropods need to shed their relatively rigid cuticle to grow (13) and it has been proposed that the evolution of this protective exoskeleton has had an antagonistic effect on the regenerative capabilities of ecdysozoans (5, 7). This implies that the potential benefits of axial regeneration for individual fitness did not contribute to the success of ecdysozoan evolution, including the unparalleled diversification of arthropods. Notably, this situation differs from many other protostome lineages, such as the likewise segmented annelid worms, which comprise many taxa with outstanding axial regenerative abilities that can be traced back all the way to the annelid ancestor (6, 14).

Discordant with the hypothesis of an ecdysozoan-wide loss of axial regeneration, however, there are some indications that the marine sea spiders (Pycnogonida) may be able to regenerate lost trunk segments (TSs) at the posterior body pole (15). Notably, this would not only be exceptional for Arthropoda (7, 9, 16) but may potentially also represent an ancestral trait, given that the pycnogonid lineage diverged near the base of the arthropod

Author affiliations: [a]Cytologie und Evolutionsbiologie, Zoologisches Institut und Museum, Universität Greifswald, Greifswald 17489, Germany; [b]Integrative Zoology, Department of Evolutionary Biology, Universität Wien, Wien 1030, Austria; and [c]Vergleichende Zoologie, Institut für Biologie, Humboldt-Universität zu Berlin, Berlin 10115, Germany

Author contributions: G.B. designed research; G.B., K.F., and L.M. performed research; G.B. and G.S. contributed new reagents/analytic tools; G.B., K.F., and G.S. analyzed data; and G.B. and G.S. wrote the paper.

The authors declare no competing interest.

This article is a PNAS Direct Submission.

[1]To whom correspondence may be addressed. Email: georg.brenneis@posteo.de.

This article contains supporting information online at https://www.pnas.org/lookup/suppl/doi:10.1073/pnas.2217272120/-/DCSupplemental.

Published January 23, 2023.

tree and forms the sister group of all other extant chelicerate taxa (horseshoe crabs, spiders, scorpions, and relatives) (8, 17, 18). Most pycnogonids are octopodous, i.e., their trunk is equipped with four leg pairs (*SI Appendix*, Fig. S1 *A*–*C*), but few extra-legged genera with five or six leg pairs exist (19). In contrast to most fossil and extant chelicerates, the pycnogonid body does not show the characteristic subdivision into a prosoma and opisthosoma (20). Rather, the ultimate leg-bearing TS bears an unsegmented anal tubercle (AT; the so-called abdomen) that contains the hindgut and features the terminally positioned anus. The nine-articled legs are penetrated by diverticula of the midgut (*SI Appendix*, Fig. S1*D*) and the gonads, with gonopores opening on the coxae 2 of one to all leg pairs (21). The pycnogonid central nervous system is composed of separate segmental ganglia (22), which likely reflects the ancestral chelicerate condition (23, 24). Given stem lineage fossils with additional limbless TSs (25, 26) and the transient formation of supernumerary posterior ganglion anlagen during pycnogonid development (27–29), the AT of extant representatives has been alternatively interpreted as largely reduced opisthosoma without telson (20, 25) or as fusion product of vestigial opisthosoma segments with the terminal telson (28).

While the leg regeneration potential of pycnogonids is well-established (27, 30, 31) (*SI Appendix*, Fig. S1), dedicated experiments aiming to clarify the presence and extent of axial regenerative capabilities in this old arthropod lineage are lacking to this day. To address this issue, we performed amputation experiments on different developmental instars and adults of the long-lived sea spider *Pycnogonum litorale* (Strøm, 1762) (Fig. 1 *A* and *B*).

Results

Normal Development of Mesodermal and Ectodermal Tissues at the Posterior Body Pole. To pinpoint the timing of mesodermal and ectodermal tissue differentiation at the posterior body pole during normal development of *P. litorale*, we studied at which developmental stage the formation of the hindgut and its associated musculature occurs in the AT anlage. Concordant with recent histology-based findings (32), fluorescent phalloidin staining of F-actin-rich structures reveals that the proctodeal dilatator muscles, which flank the hindgut and open the slit-shaped anus, as well as the proctodeal ring musculature become first detectable in late stages of postembryonic instar IV (Fig. 1 *C* and *C'*) and are well-developed from early instar V onward (Fig. 1 *D* and *D'*). Accordingly, instar V was chosen as the youngest stage for posterior amputation experiments, as successful axial regeneration would have to restore terminally differentiated mesodermal and ectodermal tissues of the AT, including the anus itself.

Survival after Posterior Amputation. A total of 23 specimens were subjected to posterior amputation (*SI Appendix*, Table S1). These animals belonged to different developmental stages, and the extent of posterior amputation varied (Fig. 2 and *SI Appendix*, Table S1), ranging from the removal of only the AT and the tips of posterior limb buds in instar V (Fig. 3 *A*–*C*) to the complete amputation of TS2 to TS4 and the AT in one juvenile (*SI Appendix*, Fig. S3*A*). Irrespective of the amputation extent, the wound expelled hemolymph only during the first minutes, after which it was closed by hemolymph coagulation. All 23 specimens survived the treatment and were actively moving in the next days. However, two of them died during the first two post-amputation weeks (Fig. 2 and *SI Appendix*, Table S1). One of these (InsV_4) appeared to be malnourished and may not have been feeding after amputation. The other was the single specimen (Juv_6) that had been subjected to TS2 to TS4 amputation, which died 4 d after the treatment during an unsuccessful molt. Another animal (InsV_5) could not be relocated after its first molt (Fig. 2 and *SI Appendix*, Table S1), which—judging by the exuvia found in the cage—appeared to have been successful. Excluding this lost specimen, the long-term survival after amputation amounts to 90.9 % (20/22).

Frequency of Posterior Axial Regeneration. The surviving specimens were continually monitored, and any molts and concurrent morphological changes were documented (Figs. 2–4 and *SI Appendix*, Figs. S2 and S3). Notably, all of the 16 long-term surviving immature animals molted at least once, but typically multiple times. With the exception of two animals, all of them initiated posterior regeneration and primordial regenerates emerged after the first molt to continue differentiation with ongoing development (Figs. 3 and 4 and *SI Appendix*, Figs. S2 and S3). Thus, posterior regeneration processes occurred in 87.5 % (14/16) of the immature specimens. By contrast, none of the four adults molted and regenerated during the course of the study. Two of them died more than 10 wk after the treatment, whereas the other two were still alive but unchanged after more than a year (Fig. 2 and *SI Appendix*, Table S1). These observations support previous suggestions of a terminal anecdysis in *P. litorale* after it reaches adulthood (33, 34), which impedes regrowth of lost body parts (34, 35). Accordingly, the structural regenerative capability of *P. litorale* seems to be restricted to its immature instars, as has been previously proposed for other pycnogonids (36).

Amputation at the TS3 to TS4 Border and through the TS4 Anlage Leads to Regeneration of TS4 and AT. To assess whether immature *P. litorale* are able to regenerate the posterior-most TS4 and the terminal AT after having attained the complete body organization, we performed transverse amputation between TS3 and TS4 on four specimens in the epimorphic growth phase (2× juvenile, 2× subadult), which internally leaves all ganglia of the central nervous system unharmed (Fig. 4*A*). After one or two molts, all four animals regenerated TS4 with a complete leg pair and the AT (Fig. 4*B* and *SI Appendix*, Fig. S3*C*). Using microcomputed X-ray Tomography (μCT) to study the internal anatomy after regeneration, we could confirm the regular array of the four ventral ganglia, the midgut diverticula, and a functional hindgut with musculature (Fig. 5 *A* and *B*).

Additionally, one specimen in the last anamorphic stage (InsVI_1) was subjected to the same treatment, with a surplus removal of the legs of TS3 (*SI Appendix*, Fig. S2 *A* and *C*). Over two molts, it regenerated leg pair 3 and TS4. However, the AT remained vestigial (*SI Appendix*, Fig. S2*C*), lacking the anus, hindgut, and its dilatator muscles.

Finally, in a penultimate anamorphic instar (InsV_6), the tips of TS3 limb buds and complete AT were removed, which also affected the interior limb primordia of TS4, but not the affiliated ventral ganglion (Fig. 3 *A* and *B*). After two molts, TS3 and TS4 were externally and internally normally formed. A vestigial AT was likewise developed (Fig. 3*B*) but had failed to differentiate the anus, hindgut, and its dilatator musculature. Five subsequent molts did not change its organization (*SI Appendix*, Fig. S4 *E* and *F*).

Amputation at the TS2 to TS3 Border Mostly Leads to Regeneration of TS3 and AT. In a second step, we tested whether more than one TS can be rebuilt by transverse amputation of all body parts posterior to TS2, which entails the removal of the posterior-most ventral ganglion 4 (Figs. 3*A* and 4*A* and *SI Appendix*, Fig. S2*A*).

In six out of the eight monitored specimens (1× InsV; 2× InsVI; 2× juvenile; and 1× subadult), posterior regeneration was initiated.

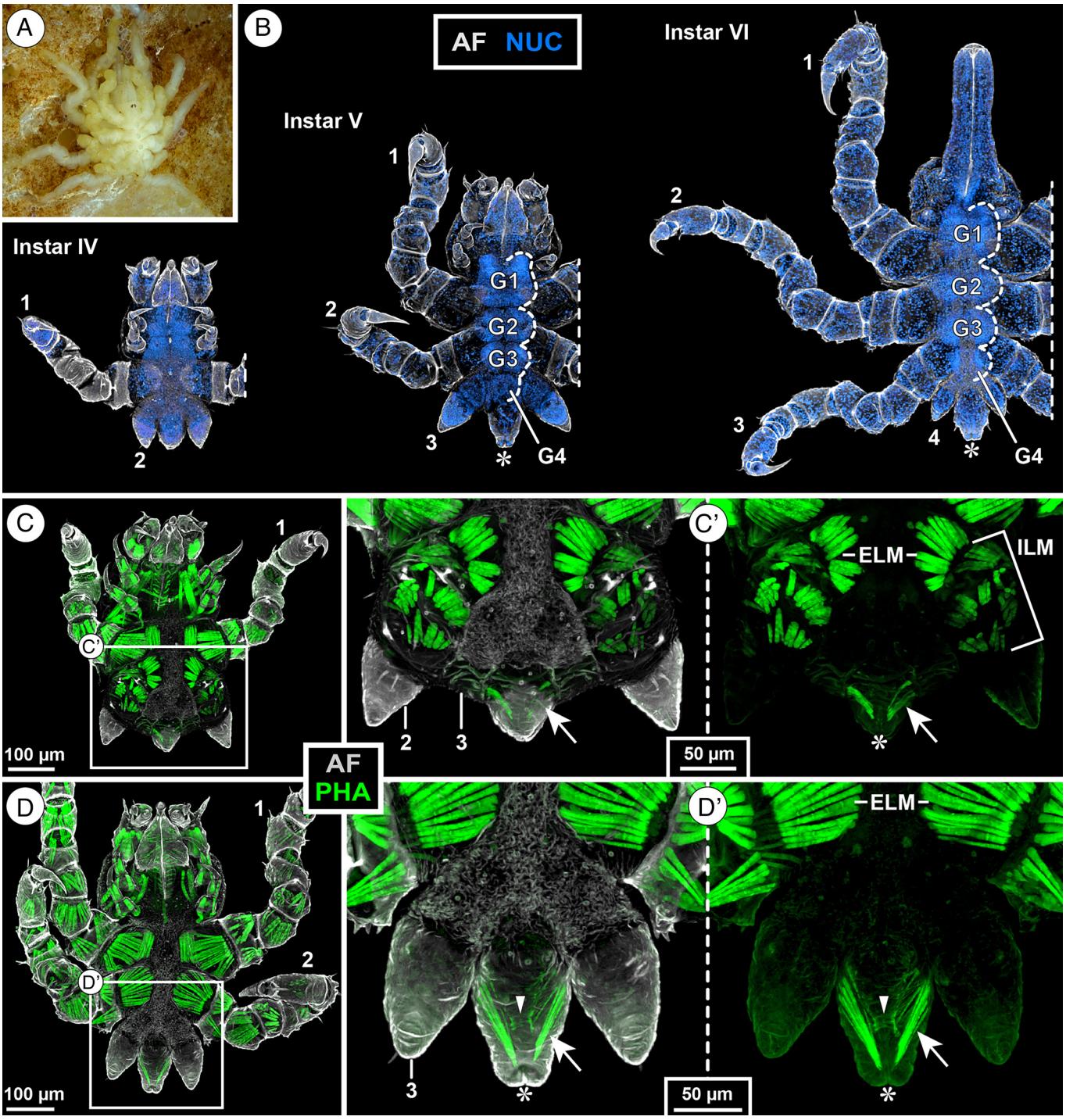

Fig. 1. Anamorphic development and hindgut differentiation in *P. litorale*. (*A*) Copulating male and female in dorsal view. (*B*) Selected instars (ventral view) illustrate the anteroposterior developmental gradient during the anamorphic post-embryonic development. (*C* and *C'*) First bundles of the hindgut dilatator musculature (arrow) and the anlage of the slit-shaped anus (asterisk) are recognizable in late instar IV (ventral view). (*D* and *D'*) Proctodeal dilatator muscles (arrow), ring musculature of the through-gut (arrowhead) and the open slit-shaped anus (asterisk) are well-developed in instar V (ventral view). AF, cuticular autofluorescence; ELM, extrinsic leg muscles; G1-4, ventral ganglia 1 to 4; ILM, intrinsic leg muscles; NUC, nuclear staining; PHA, phalloidin labeling; 1 to 4, leg pairs 1 to 4.

Four of the younger instars regenerated TS3 with completely articulated legs and a fully developed AT in the course of two molts (Figs. 3*D* and 4*D* and *SI Appendix*, Figs. S2*B* and S4*C*). Notably, however, TS4 was not formed, resulting in hypomeric, six-legged specimens. While these hypomeric animals consistently feature a functional through-gut with dilatator muscles of the hindgut (*SI Appendix*, Fig. S4*D*), the ventral ganglion 4 is missing, concomitant to the lack of TS4 with its leg pair (*SI Appendix*, Fig. S4*D*). Interestingly enough, these results provide plausible causal explanations for hypomeric, six-legged specimens previously reported in field-collected pycnogonids (37, 38). Hitherto, potential causes leading to such forms were obscure, but our experiments now demonstrate that TS3+4 loss in immatures—for instance, due to predation—followed by incomplete posterior axial regeneration may account for this phenotype.

One juvenile of this experimental batch (Juv_3) displayed a bilaterally asymmetrical regeneration pattern, leading after three molts to a seven-legged final body organization. In addition to

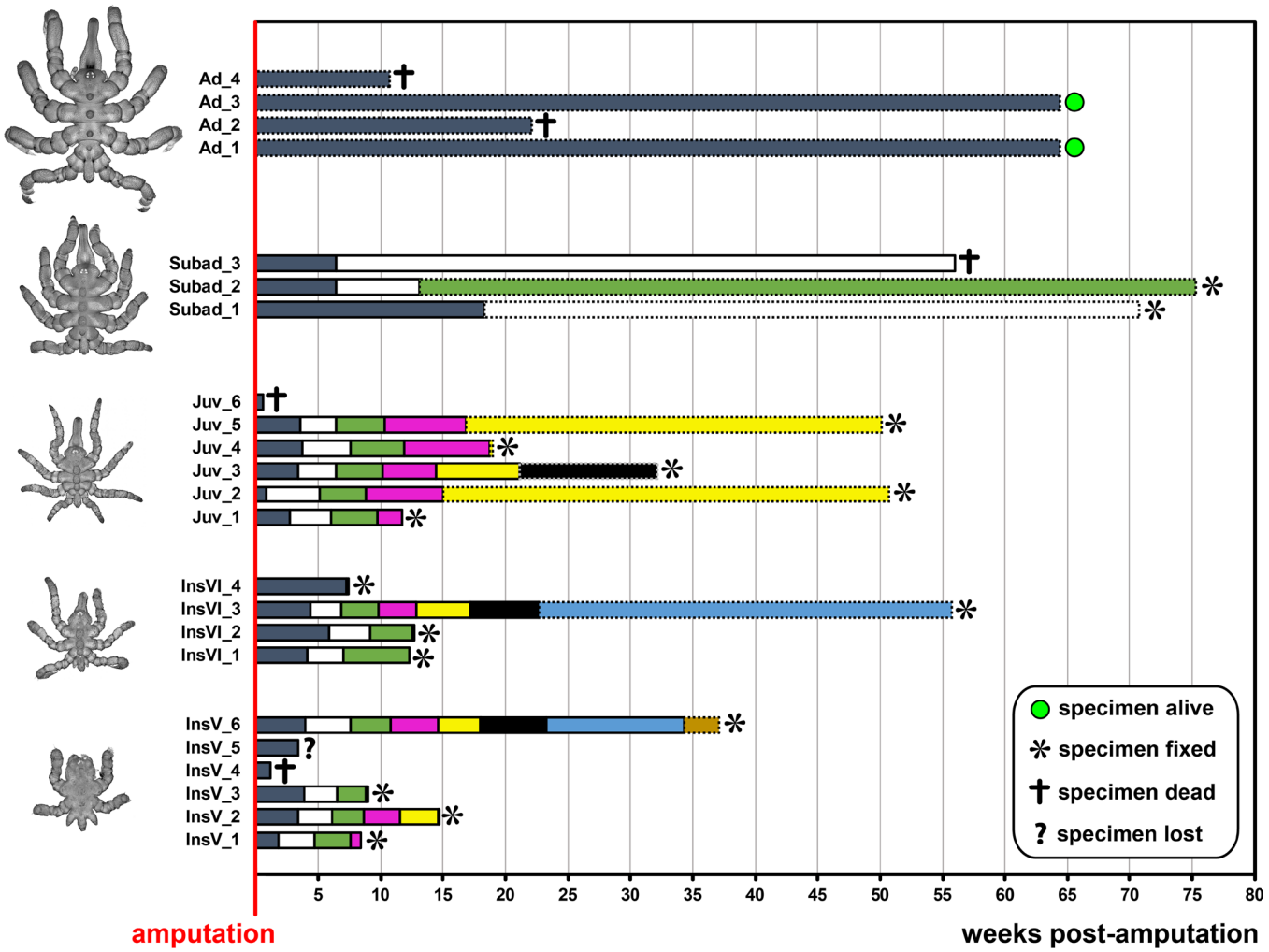

Fig. 2. Survival and molting of experimental animals after posterior amputation. Specimens in four immature developmental stages and adults were included in the amputation experiments (left side). The horizontal bars represent single individuals. At the border between differently colored sections of a single bar, the specimen underwent a molt. The stippled outlines of bar sections at the far right indicate that experimental animals reached maturity.

TS3, the left half of TS4 was regenerated, being flanked on its right side by the newly formed AT (Figs. 4*D* and 5*C*). Its hindgut is normally developed and displays the characteristic proctodeal dilatator musculature (Fig. 5 *D*–*F*). Deviating from the normal arrangement, however, the unpaired leg 4 is innervated by two nerves emanating from ventral ganglion 3 and its gut diverticulum branches off the diverticulum of the left leg 3 (Fig. 5 *D* and *F*). In correspondence to the six-legged forms, a previously described seven-legged female of *P. litorale* collected in the wild closely resembles our amputation-induced seven-legged phenotype (39).

The single subadult specimen subjected to this amputation treatment (Subad_3) molted only once (*SI Appendix*, Fig. S3*B*), followed by a 50-wk-intermolt period terminating in its death (Fig. 2). It regenerated only a shallow posterior protrusion and a small bud that may have represented an early limb bud stage (*SI Appendix*, Fig. S3*B*).

Notably, two of the eight specimens subjected to the treatment did not show posterior regeneration (Fig. 3*D* and *SI Appendix*, Fig. S2*B*). While one of them (InsVI_4) was directly fixed after its first molt, the other one (InsV_1) was monitored for two additional molts, which did not result in further changes at the posterior pole (Fig. 2 and *SI Appendix*, Fig. S4*A*). Accordingly, both animals lack the TS3, TS4, AT, and anus (Fig. 3*D* and *SI Appendix*, Fig. S2*B*). In line with this, μCT analysis of the specimens revealed a blind-ending midgut and the lack of posterior ganglia (*SI Appendix*, Fig. S4*B*). Despite the absence of a through-gut, the animals were actively feeding and occasionally observed to regurgitate gut contents.

Amputation with Oblique Cutting Plane Leads to Bilaterally Symmetrical Regeneration Patterns. The previous experiments resulted in a bilateral anteroposterior regeneration pattern. To assess how regeneration patterns are affected by a bilaterally asymmetrical loss of body parts, we subjected two individuals to posterior amputation with an oblique cutting plane.

One juvenile (Juv_2) was obliquely amputated between TS3 and TS4, so that not only the complete TS4 but also the right half of TS3 was partly removed (Fig. 4*C*), without affecting the ventral ganglia. After 6 d, it molted for the first time (Fig. 2) without external signs of regeneration, but subsequently regenerated the amputated body parts in the course of the two following molts, concomitant with a normal arrangement of ganglia, gut diverticula, hindgut, and dilatator muscles.

In anamorphic InsV_2, the AT, the right side of the TS4 anlage and the right limb bud of TS3 were obliquely amputated (Fig. 3 *A* and *C*). After two molts, this specimen had formed a normal TS3 with legs, that was additionally equipped with a dorsally inclined AT and an aberrant, posteroventrally projecting unpaired leg anlage with a distal bifurcation (Fig. 3*C*). This transient phenotype shows

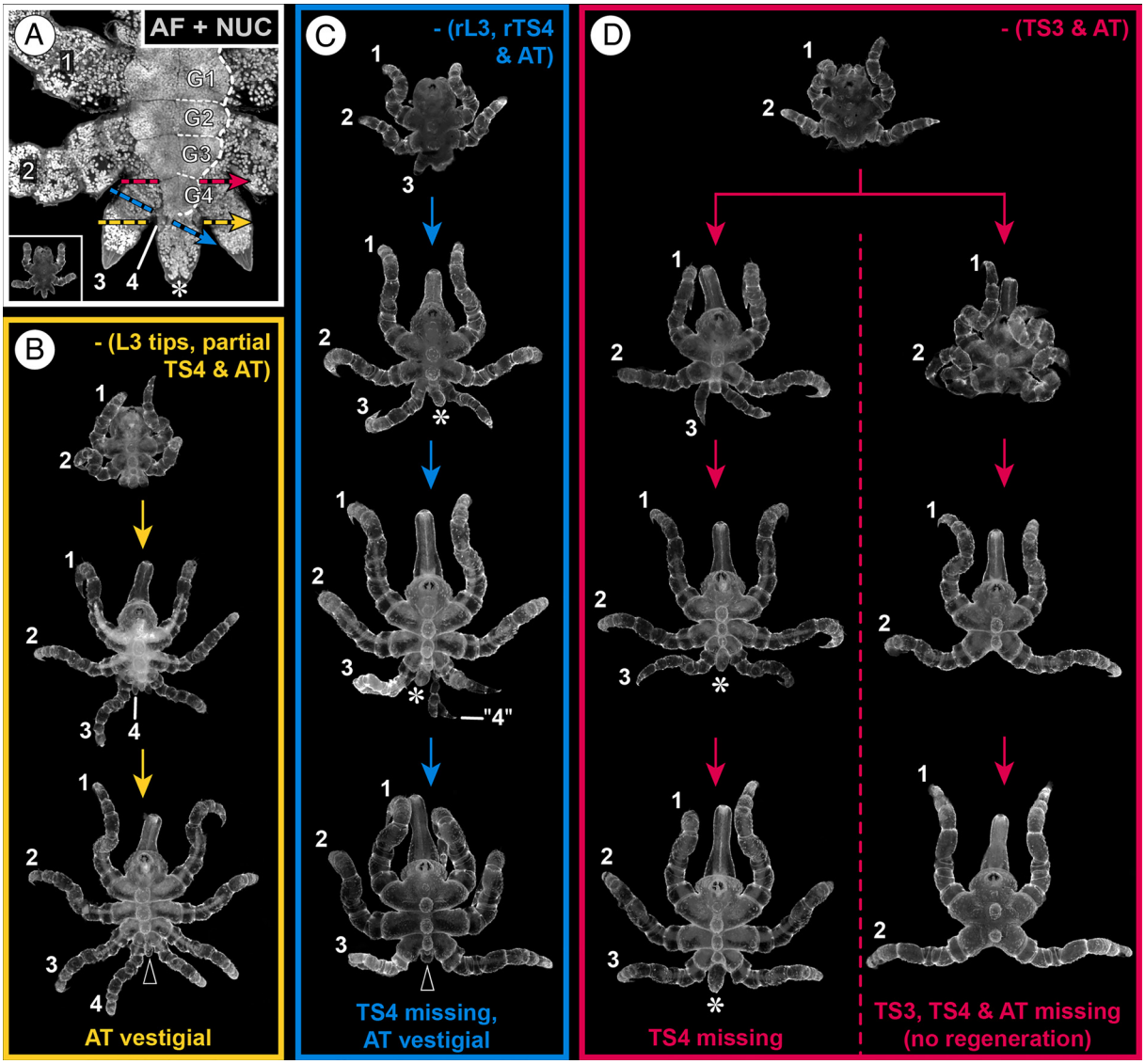

Fig. 3. Axial regeneration patterns in anamorphic instar V. (*A*) Ventral detail of instar V depicting the different section planes (colored arrows, colors matching with details shown in *B*–*D*) in the posterior amputation experiments. The small inset in the *Left Bottom* corner shows instar V in dorsal view. (*B*) After partial removal of the primordial fourth TS and the AT, an eight-legged phenotype with vestigial AT (arrowhead) is formed (*SI Appendix*, Fig. S4 *E* and *F*). (*C*) Oblique amputation affecting the AT, the TS4 primordium and the right limb bud of TS3 resulted in the transient regeneration of an AT (asterisk) and an aberrant bifurcating leg 4 ("4", *SI Appendix*, Fig. S5 *A*–*F*). After shedding of both regenerated structures with the next molt, a hypomeric, six-legged phenotype with vestigial AT (arrowhead) is formed. (*D*) Transverse amputation at the TS2 to TS3 border results in no regeneration (right column; *SI Appendix*, Fig. S4 *A* and *B*), or a hypomeric, six-legged phenotype (left column; *SI Appendix*, Fig. S4 *C* and *D*) with anus-bearing AT (asterisk). AF, cuticular autofluorescence; G1-4, ventral ganglia 1 to 4; L, leg; NUC, nuclear staining; r, right; 1 to 4, leg pairs 1 to 4.

striking similarities to previous reports of pycnogonids with posteriorly directed bi- or tri-furcating legs (30, 40). With the third molt, however, the AT and aberrant leg were shed (*SI Appendix*, Fig. S5 *C* and *D*), leaving only a tiny posterior protrusion without anus (Fig. 3*C*). Two subsequent molts did not result in further changes of this body organization (*SI Appendix*, Fig. S5*A*) and similar to the other six-legged phenotypes, the specimen lacks ventral ganglion 4 (*SI Appendix*, Fig. S5*B*). Instead of a through-gut, it features only a tiny posterior midgut protrusion that ends blindly in TS3 (*SI Appendix*, Fig. S5*B*). Micro-CT analysis of the exuvia shed with the third molt reveals a slit-shaped anus, proctodeal musculature, and the characteristic distal ampulla of the gut in the AT (*SI Appendix*, Fig. S5*E*), demonstrating that the initial regeneration resulted in the differentiation of correct AT structures. Also, the misdeveloped unpaired leg anlage contained tissues, including muscle fibers (*SI Appendix*, Fig. S5*F*), but the bad tissue condition indicates an onset of degradation prior to the molt.

Ectopic Reproductive Structures in Regenerated Legs. In contrast to most other pycnogonids, only the ultimate leg pair 4 of *P. litorale* develops gonoducts and gonopores (32). To assess whether the posterior regenerative processes also include the respecification and correct development of these distal reproductive structures and thereby reestablish the functionality of the reproductive system, we monitored eight of the experimental animals until full maturation (Fig. 2).

After partial amputation of the TS4 primordium and the AT in anamorphic instar V (n = 1; InsV_6), a regular pair of gonopores is present on the fully formed leg pair 4 of the mature adult (*SI Appendix*, Fig. S4*F*).

Following amputation at the TS3 to TS4 border (n = 3), two of the experimental specimens (Juv_4, Subad_2) formed gonopores on the regenerated leg pair 4, targeted by gonoducts and equipped with regular gonopore musculature (Fig. 5*B*). The third specimen was a subadult female that molted only once after the amputation

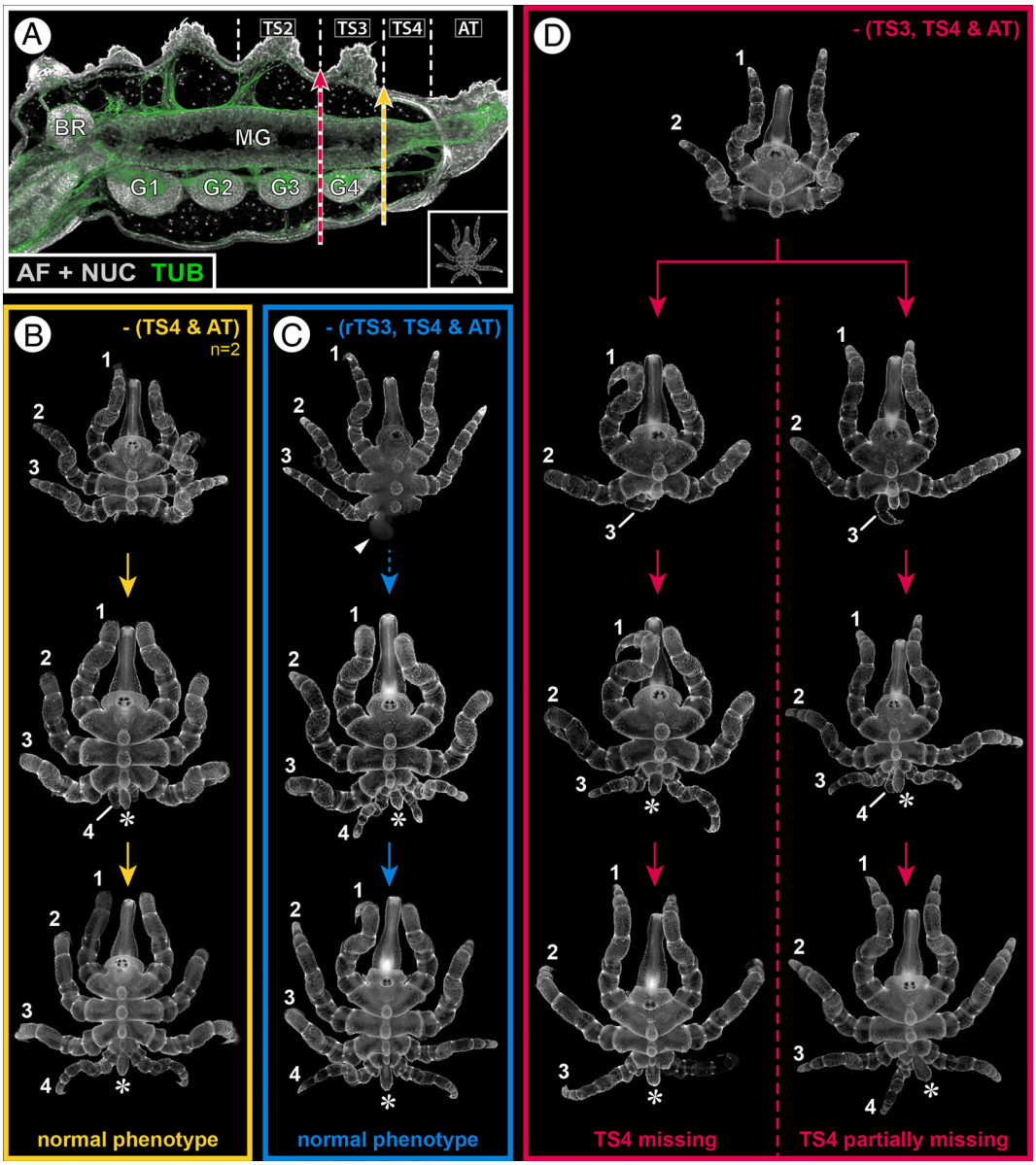

Fig. 4. Axial regeneration patterns in epimorphic juvenile instars. (*A*) Sagittal extended optical section through a juvenile (anterior to the left) illustrating two of the three different section planes (colored arrows, colors matching with details shown in *B* and *D*) in the amputation experiments. The small inset in the *Right Bottom* corner shows a juvenile in dorsal view. (*B*) After removal of the ultimate leg-bearing TS and the AT (asterisk), a normal eight-legged phenotype is formed after two molts. (*C*) After oblique amputation of the AT, TS4 and part of the right TS3 half, a normal phenotype is likewise restored. Note coagulating hemolymph at the wound site after the amputation procedure (white arrowhead). The stippled blue arrow indicates an additional molt that is not shown. (*D*) Transverse amputation at the TS2 to TS3 border resulted in a hypomeric, six-legged phenotype with anus-bearing AT (left column) and a seven-legged specimen with normal AT. AF, cuticular autofluorescence; BR, brain; G1-4, ventral ganglia 1 to 4; L, leg; MG, midgut; NUC, nuclear staining; r, right; TUB, tubulin immunolabeling; 1 to 4, leg pairs 1 to 4.

(Subad_1, Fig. 2). Although its regenerated leg pair 4 remained smaller than normal and did not develop any gonopores, the presence of mature oocytes in the trunk and other leg pairs indicate that it had reached maturity.

After amputation at the TS2 to TS3 border (n = 3), the two monitored six-legged specimens (InsVI_3, Juv_5) and the one seven-legged specimen (Juv_3) displayed an untypical pattern. Regenerated legs of TS3 may bear ectopic gonopores with associated musculature and regular gonoduct but not necessarily in both body halves (Fig. 5 *E* and *F* and *SI Appendix*, Fig. S5*G*). Moreover, even if the gonopore itself and its musculature are not formed in the regenerated leg 3, a gonoduct may still target the inner side of the coxa 2 cuticle.

Oblique amputation of TS4 and one half of TS3 (n = 1; Juv_2) resulted likewise in the ectopic formation of a slightly smaller gonopore with gonoduct in the regenerated leg 3, in addition to the normal pair of gonopores on leg pair 4 (*SI Appendix*, Fig. S5*H*).

Discussion

Sea Spiders Can Regenerate Almost Complete Segments and the Posterior Body Pole. Prior to this study, the only indications for posterior axial regeneration in arthropods stem from some amputation experiments on insect larvae and pycnogonids from the turn of the 19th to the 20th century (16, 41, 42). However, these studies suffered from extremely high mortality rates of treated animals, as well as often only partial ablation of terminal segments or insufficient characterization of the regenerated structures' internal anatomy. Consequently, the nature of the

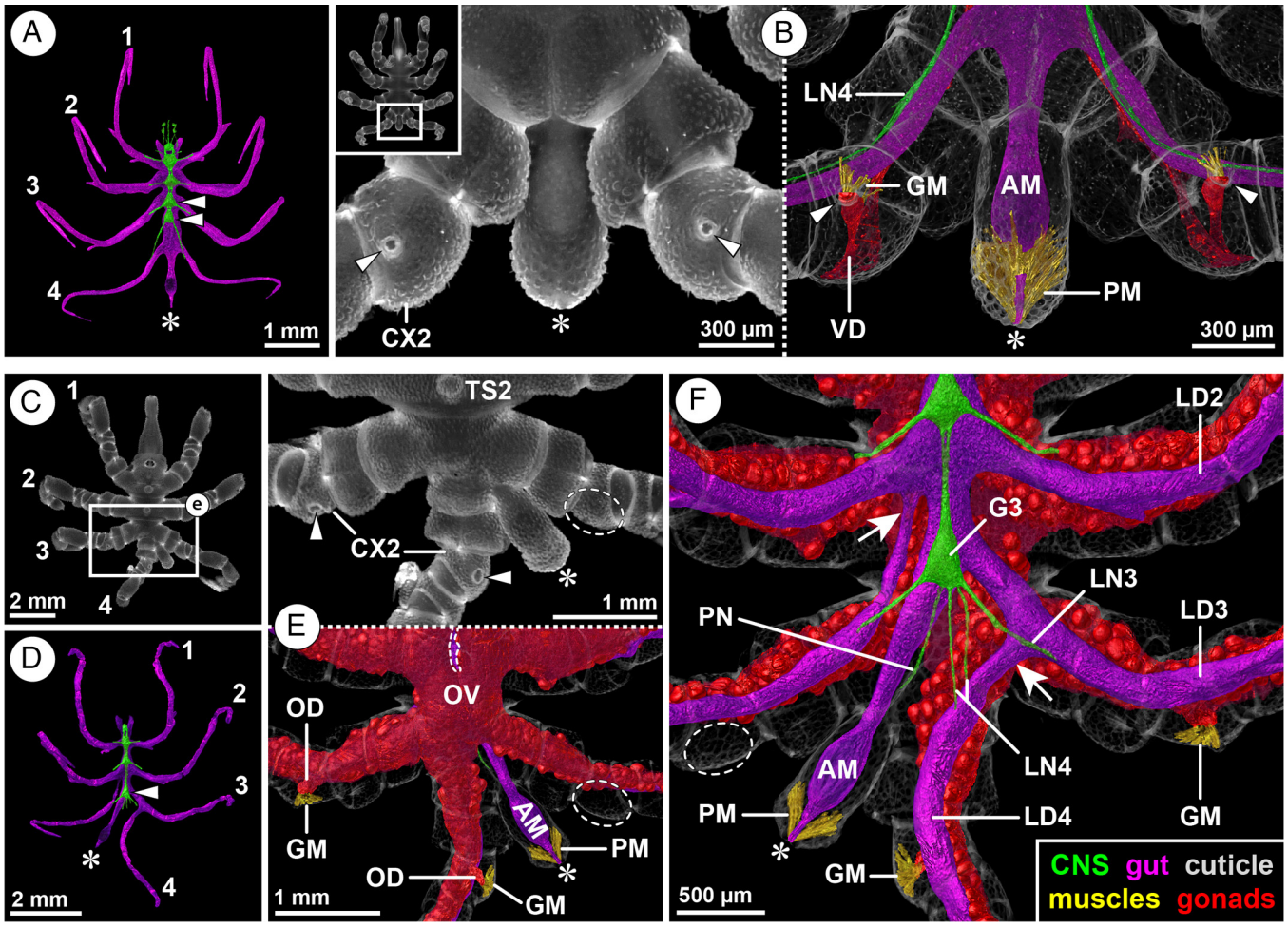

Fig. 5. Internal anatomy of experimental animals after reaching maturity. (*A* and *B*) Adult male specimen (Juv_4), four molts after amputation at the TS3 to TS4 border, ventral views. (*A*) The normal phenotype has regenerated, with midgut diverticula (1 to 4) in all four leg pairs, the hindgut with slit-shaped anal opening (asterisk), and a complete ventral nerve cord (arrowheads mark ganglia 3 and 4). (*B*) The regenerated leg pair 4 displays regular ventral gonopores (arrowheads), targeted by vasa deferentia and equipped with gonopore muscles (GM). The slit-shaped anus (asterisk) is opened by regular proctodeal dilatator musculature (PM). (*C*–*F*) Adult female specimen (Juv_3), five molts after amputation at the TS2 to TS3 border, dorsal (*C* and *E*) and ventral (*D* and *F*) views. (*C*) A hypomeric, seven-legged phenotype has formed. (*D*) All legs are penetrated by midgut diverticula (1 to 4) and the hindgut with slit-shaped anal opening (asterisk) is regenerated, but ventral ganglion 4 is missing (arrowhead highlights ganglion 3). (*E*) While a gonopore (arrowhead) connected with a regular oviduct (OD) and gonopore musculature (GM) is present on the two regenerated legs in the left body half, it is lacking on the right leg 3 (stippled oval). (*F*) The nerves targeting the unpaired leg 4 and the proctodeum (LN4 and PN, respectively) emanate from the posterior side of ventral ganglion 3 (G3). The midgut diverticula of the right leg 3 and of the unpaired leg 4 branch off at untypical locations (arrows). AM, distal gut ampulla; CX2, coxa 2; LD, leg diverticulum; LN, leg nerve; OV, ovary; VD, vas deferens.

de novo formed body parts has remained ambiguous. In the case of pycnogonids, this has led to a debate between the two famous experimental biologists Jacques Loeb and Thomas Hunt Morgan regarding the interpretation of a regenerated structure in *Phoxichilidium femoratum* (Rathke, 1799) either as a posteriorly directed malformed leg or as newly formed posterior TSs (15, 36). More than a century after this unresolved discussion, our study not only demonstrates remarkable resilience to traumatic injury in the sea spider *P. litorale* but unequivocally confirms that posterior axial regeneration is a common phenomenon in its immature specimens. In contrast to our results, Loeb and Morgan failed to follow the regeneration processes until complete differentiation in their pioneering experiments. This was likely due to suboptimal experimental conditions, as the animals were kept in sea water-filled petri dishes without food (15, 36). Given that starvation is one of the key factors known to cause significant molting delays in juvenile sea spiders (34), insufficient nutrition likely accounts for the low frequency of molting and posterior regeneration encountered in the previous studies.

Our results leave no doubt as to the identities of the de novo-formed structures and reveal that sea spiders are capable of rebuilding a functional terminal body region as well as almost complete segments comprising the majority of the serially iterated structures along the main body axis, such as a body ring, fully articulated legs with musculature and leg nerves, and the diverticula of the midgut and the gonads. Hence, the axial regeneration patterns in pycnogonids show a degree of complexity hitherto unknown for arthropods, with several correspondences to those of some annelid taxa (6, 14). This challenges the prevailing dogma of the virtual absence of axial regeneration in arthropods (5, 6, 9), which has been alternatively suggested to be causally linked to the early determination of the body poles during arthropod embryogenesis (12) or to the evolution of the rigid exoskeletal cuticle that necessitates molting (5, 7). Our findings refute the validity of these explanation attempts for arthropods as a whole and should serve as an incentive for rigorous reinvestigations of the regenerative potential in more arthropod taxa.

The Extent of Trunk Regeneration Relies on the Presence of Segmental Ganglia. Anterior to the AT, the trunk displays amputation plane-dependent regeneration patterns. In this context, our results point to the presence or absence of segmental ventral

ganglia as a potential key factor for TS regeneration. In *P. litorale*, the ventral ganglia are forward-shifted in relation to the external TS borders (22, 32). Consequently, transverse amputation at the TS3–TS4 border does not affect ganglion 4 and its segmental nerve roots, correlating with the subsequent complete regrowth of the remaining TS4 elements. By contrast, amputation at the TS2 to TS3 border entails the loss of ganglion 4, and neither the ganglion itself nor the remaining elements of TS4 are reformed (although the AT is), leading to hypomeric, six-legged phenotypes. A notable exception to this pattern is the seven-legged specimen with a one-sided leg 4. But also in this case, ganglion 4 failed to regenerate and the unpaired leg 4 is innervated by ganglion 3 instead. Together with the aberrant origin of the unpaired leg's gut and gonad diverticula from the ones of leg 3, this innervation points to a duplication of the left half of TS3 as a consequence of irregular regeneration, rather than partial regeneration of a regular TS4.

An intact nerve supply at a wound site and concomitant nerve-dependent signaling is known to be key for reparative regeneration processes in many animal taxa (43, 44), including limb regeneration in vertebrates (45) and potentially in arthropods (2, 46), as well as body segment regeneration in annelid taxa (47–49). However, while many annelids readily replace complete body segments with their ganglia as long as the wound region contains some nervous tissue, pycnogonids seem to regrow only the missing serial structures of those segments of which the ganglia and their nerve roots have not been affected by the injury. In contrast to annelids, this renders the restored pycnogonid segments a mosaic of previously existing and de novo-formed elements.

A New Hypothesis on the Nature of the Pycnogonid AT. The pycnogonid AT has been interpreted as a strongly reduced chelicerate opisthosoma without a telson (20, 25) or as a fusion product of vestigial opisthosoma segments and the anus-bearing telson (28). This has been deduced from the ubiquitous occurrence of an opisthosoma in the other Chelicerata [including pycnogonid stem lineage representatives (25, 26)] and from one or two transient ganglion anlagen found during pycnogonid development, posterior to the ventral ganglion that targets the ultimate leg pair (27–29).

Notably, however, we here document complete AT regrowth even in hypomeric animals that failed to regenerate the ultimate TS4. This strongly suggests that the AT does not comprise any segmental elements but rather represents the asegmental terminal telson only. Further support for this interpretation may be derived from a comparison with posterior regeneration patterns in the segmented annelids. Here, regrowth and differentiation of the asegmental, anus-bearing pygidium predate the restoration of segmental structures anterior to it (6, 48, 50), and the number of segments that are eventually regenerated may vary and fall short of the preamputation state (14). Accordingly, regeneration of the asegmental terminal pygidium of annelids mirrors the situation in pycnogonids, where the restoration of the terminal AT is decoupled from the number of regrown segmental structures. If the entire AT corresponds to the asegmental telson, the transient posterior ganglion anlagen formed during development (27, 28) suggest the inclusion of vestigial opisthosoma segments in stem lineage representatives into the ultimate TS of crown group pycnogonids. This hypothesis is supported by the observation that these transient ganglion anlagen fuse into the posterior side of the ultimate leg ganglion of adult pycnogonids (23).

Ectopic Gonopore Formation May Rescue Reproductive Functionality. Normally, gonoducts and gonopores are exclusively formed by the ultimate leg pair in *P. litorale* (32). Unexpectedly, we found that not only regenerated leg pairs 4 differentiate these structures after posterior amputation, but also the ultimate leg pair 3 in hypomeric phenotypes, even if not in all cases completely. Consequently, even failure to regenerate TS4 after loss of TS3+4 does not necessarily impede successful reproduction of hypomeric specimens, as the functionality of their reproductive system is reestablished by ectopic formation of its distal elements in TS3.

To date, the gene regulatory networks governing posterior axis patterning and elongation, segmentation, and segmental identity are virtually unstudied in pycnogonids. In spite of this, our findings strongly indicate that specification and differentiation of the distal reproductive structures in *P. litorale* are instructed by signaling from the developing posterior body pole, rather than being predefined for a specific TS number. Further support for a posteriorly instructed identity of the gonopore-bearing TS in pycnogonids may be derived from the polymeric genus *Pentapycnon*, which is closely related to *Pycnogonum* (18) and features five instead of four leg-bearing TSs (19). Concordant with *Pycnogonum*, the gonopores of *Pentapycnon* are exclusively formed on the ultimate leg pair 5, whereas the penultimate leg pair 4 lacks them (51, 52).

Is Posterior Axial Regeneration an Ancestral Feature of Arthropoda? As the sister group of all other extant chelicerates (8, 17) with a Paleozoic onset of crown group diversification (18, 53), the primary marine sea spiders can help to illuminate early chelicerate and arthropod evolution. Notably, within pycnogonids, the anamorphic development of *P. litorale* likely represents the ancestral developmental pathway (54), aligning with the hypothesized plesiomorphic anamorphic development via a segment-poor hatching stage in the marine arthropod ancestor (55, 56). Hence, by extension from pycnogonids, this suggests that also representatives of the marine arthropod stem group may have exhibited similar resilience to traumatic posterior segment loss followed by axial regeneration, which increased individual survival and reproduction success and thus contributed to the successful early radiation of the arthropod lineage. To put this hypothesis to the test, modern regeneration studies on other arthropod taxa as well as nonarthropod ecdysozoans (other than nematodes) are needed. Recent advances in functional and comparative genomics have led to a significantly better characterization of the cellular and molecular basis of regeneration in various invertebrate lineages (4, 57). With comparative investigations of more nonmodel protostome taxa, these approaches have the potential to inform the long-standing debate whether and at what level regenerative processes are homologous across the various taxa (12, 57, 58). This concerns also the open question of whether the pattern similarities of pycnogonid and annelid axial regeneration i) reflect a shared inheritance of this trait from the protostome ancestor or rather ii) constitute a by-product of the restoration of a segmented body organization, which likely evolved independently in arthropods and annelids (59).

Materials and Methods

Choice of Experimental Animal. *P. litorale* was chosen as the experimental animal for several reasons: i) It is long-lived and can be kept together with its prey in reproducing laboratory cultures (60). This permits long-term experiments under controlled conditions with optimal food supply. ii) Deviating from most other pycnogonids, *P. litorale* possesses only one pair of gonopores on its ultimate leg pair 4 (32). Hence, if posterior trunk regeneration were to occur, not only the overall body plan but possibly also the normal segmental identity of regenerated posterior legs can be assessed. iii) The postembryonic development of *P. litorale* follows the most common mode in pycnogonids (54) and is well-documented (32, 61), permitting experimental targeting of defined developmental stages. Starting from a minute hatching protonymphon larva, a stereotypical series of

six anamorphic molts with successive segment differentiation at the posterior body pole (Fig. 1*B*) leads to the first juvenile instar. This instar already shows the overall adult body organization (32) (Fig. 2) and passes through an epimorphic growth phase including five to seven additional molts before reaching maturity (61), with advanced larger juveniles being here referred to as subadults (54).

Animal Collection and Laboratory Husbandry. Adult and juvenile specimens of *P. litorale* were collected during low tide in the rocky intertidal of the German offshore island Helgoland (North Sea), transferred to Greifswald University, and maintained in artificial seawater (ASW) tanks (ca. 30 ‰ salinity, 16 to 18 °C) equipped with a recirculating filter system. The actinian *Metridium senile* (Linnaeus, 1761)–one of the preferred preys of adult and juvenile *P. litorale*–and colonies of the hydrozoan *Clava multicornis* (Forsskål, 1775)–the prey of the first five postembryonic instars–were obtained from the Biologische Anstalt Helgoland (Alfred-Wegener-Institute for Polar and Marine Research). The pycnogonids were kept in mixed female–male groups in breeding cages (16.5 × 12.5 × 13 cm) together with 2 to 4 polyps of *M. senile*. At least twice per week, cages were checked for males carrying egg batches, which were stripped of the ovigers with fine forceps and subsequently reared in separate ASW-containing plastic containers under continuous aeration. Upon hatching of the protonymphon larvae, small pieces of the batches were placed on colonies of *C. multicornis*, which were grown on plastic plates (ca. 10 × 8 cm) and fed once or twice per week with freshly reared nauplius larvae of *Artemia salina* (Linnaeus, 1758). After attachment of the protonymphon larvae to their prey, the *C. multicornis* colonies were checked daily under a stereomicroscope to monitor the postembryonic development. Following their fifth molt, instars VI were removed from the colonies and placed in breeding cages to prey on *M. senile* during the juvenile developmental phase.

Adult and juvenile specimens of *Endeis spinosa* (Montagu, 1808) were collected in the rocky intertidal at Station Biologique de Roscoff (Bretagne, France) in July 2019.

Amputation Experiments, Monitoring of Survival, and Documentation of Regeneration. *P. litorale* specimens selected for amputation experiments were anesthetized in petri dishes containing freshly carbonated ASW produced with a SodaStream sparkling water maker. After relaxation, amputation was performed with surgical microscissors under a stereomicroscope. Animals were photographed after surgery and placed in petri dishes with untreated ASW to recover. Once recovered (usually after 5 to 10 min), they were placed in cages with *M. senile* and individually monitored on a daily basis. Deviating from this procedure, the minute instars V were amputated while attached to the stolons of *C. multicornis* and directly photographed and monitored on the plastic plates. Only after their molt to instar VI, they were transferred into cages with *M. senile*. Following each new molt, experimental animals were anesthetized, photographed, and returned to the cages.

Images of the experimental animals were taken with a Nikon SMZ25 stereomicroscope coupled to a Nikon DSRi2 camera. Z-stacks were generated with the complementary NIS Elements AR software (ver. 4.51, Nikon Corporation, Tokyo, Japan; RRID:SCR_014329). The stacks were i) either directly combined into an image with extended depth of field or ii) exported as tiff-files and subsequently merged using Helicon Focus software (ver. 6.7.1, Helicon Soft, Kharkiv, Ukraine; RRID:SCR_014462). In addition to brightfield images, the green autofluorescence of the cuticle of *P. litorale* when exposed to blue light (62) was used to document the external morphology of regenerated structures, as it permits ready identification of the number of leg articles and the presence of gonopores.

Live images of the *P. litorale* copula and of *E. spinosa* specimens were taken with a Nikon D7100 digital camera equipped with a Nikon AF-S Micro Nikkor 105 mm lens.

Microcomputed X-ray Tomography. To complement the external morphology, the experimental animals were individually fixed after completion of regeneration, and their internal anatomy was subsequently analyzed in μCT scans. For this purpose, animals were fixed and stored in Bouin's fluid (10% formaldehyde, 5% glacial acetic acid in saturated aqueous picric acid) at room temperature (RT). Specimens were briefly rinsed in phosphate-buffered saline (PBS; 1.86 mM NaH_2PO_4, 8.41 mM Na_2HPO_4, 175 mM NaCl, pH 7.4; at least 3× 5 min), transferred into deionized water, dehydrated via an ascending ethanol series, incubated in a tissue contrasting solution of 2% iodine (resublimated; Carl Roth; #X864.1) in 99.5% ethanol for 48 h at RT, rinsed in 99.5% ethanol (3 to 4× 10 min), and critical point-dried with a Leica EM CPD300. Dried specimens were placed in plastic tubes for overview scans. For higher resolution scans of the posterior body region with the regenerated structures, they were subsequently attached to plastic welding rods with hot glue. Scans were performed with an Xradia MicroXCT-200 (Carl Zeiss Microscopy) under 40 kV/200 μA/8 W or 30 kV/200 μA/6 W settings. Depending on the specimen size and region of interest, a 4×, 10×, or 20× objective was chosen. Exposure times were individually adjusted for each scan, ranging from 0.75 to 6.5 s. To reduce noise, binning 2 was applied during data acquisition. Tomography projections were reconstructed with the XMReconstructor software (Carl Zeiss Microscopy) with binning 1 (= full resolution) and TIFF format image stacks as output.

Fluorescent Histochemistry and Immunohistochemistry. Post-larval and juvenile instars were fixed for 1 h in 4% paraformaldehyde in PBS (PFA/PBS; 16% methanol-free formaldehyde [Electron Microscopy Sciences, #15710] diluted 1:4 in PBS) at RT. Prior to staining, cuticle and tissue permeability was improved by bath ultrasonication (5 to 10 brief pulses) followed by incubation in PBTx (PBS + 0.5% Triton X-100) for 2 h at RT.

For visualization of the musculature, F-actin labeling of whole specimens was performed with TRITC-conjugated phalloidin (Sigma-Aldrich, #P1951, 50 μg/mL in PBTx; RRID:AB_2315148) overnight at 4 °C, in adaptation of previous staining protocols for pycnogonids (40). After inspection of the staining quality by epifluorescence stereomicroscopy, incubation was variably extended to maximally four nights at 4 °C.

To visualize cytoskeletal microtubules, a monoclonal mouse primary antibody (anti-ac-α-tub IgG 2b Isotype, clone 6-11 B-1, Sigma-Aldrich, #T6793; RRID:AB_477585) was applied in conjunction with a Cy3-coupled secondary goat antibody (anti-mouse IgG (H+L), Jackson ImmunoResearch Labs, #115-165-146; RRID:AB_2338690). The primary antibody was raised against acetylated alpha-tubulin of the sea urchin *Strongylocentrotus purpuratus* (Stimpson, 1857). Acetylation is a common post-translational modification of alpha-tubulin in which an acetyl group is reversibly added to Lys40, representing a prominent feature of stable microtubule assemblies (63). The antibody's suitability to label cytoskeletal microtubules and thus visualize the microtubule-rich nerves and tracts of the central nervous system has been previously confirmed for pycnogonids (28, 29). Prior to antibody incubations, specimens were blocked in PBTx + 1.5% dimethyl sulfoxide + 5% normal goat serum (Thermo Fisher Scientific, #31873). Antibodies were diluted 1:200 in PBTx + 1.5% dimethyl sulfoxide; incubation times lasted 72 to 120 h and were followed by rinsing in PBTx with gentle rotation for at least 6 h at RT, with occasional extension overnight at 4 °C. Omission of the primary antibody in the procedure resulted in complete loss of signal.

For nuclear staining, the DNA marker Hoechst (H33342, Invitrogen Molecular Probes® #H1399, 1 μg/mL in PBS) was applied. Incubation lasted minimally 1 h at RT and was occasionally extended overnight at 4 °C.

After final rinsing in PBS, specimens were transferred to Vectashield® Mounting Medium (Vector Laboratories, Inc. #H-1000; RRID:AB_2336789) and mounted on microscopic slides. Tiny pieces of plasticine pieces were attached to the coverslip corners to avoid sample compression.

Confocal laser scanning microscopy (CLSM) was performed with a Leica DMI 6000 CS microscope coupled to a Leica TCS SP5 II scan unit (RRID:SCR_018714). Laser lines were chosen according to the excitation spectra of the fluorescent markers (405 nm for Hoechst and cuticular autofluorescence; 543 nm for Cy3 and TRITC), the Z-increment between optical planes ranging from 1.5 to 2 μm.

CLSM and μCT Data Analysis, 3D Reconstruction, and Data Presentation. The CLSM image stacks were analyzed and visualized in Imaris (ver. 7.00; Bitplane AG, Zurich, Switzerland, RRID:SCR_007370). Snapshots show 3D volume renderings in maximum intensity projection.

The μCT image stacks were analyzed with the software package Amira (version 5.6; FEI Visualization Sciences Group; RRID:SCR_007353) and visualized in a similar fashion as previously described (22). In brief, organ systems were manually segmented as different materials and visualized as texture-based 3D volume renderings (module "Volren", mode "VRT") with specular shading. Color and transparency of the 3D volume renderings were defined by adjusting the color field and alpha-scale values of each material's transfer function. As an external morphological reference system, the unsegmented structures of the data stacks are shown in semitransparent grayscale values. To ensure the visibility of internal structures, filtered oblique slicers were selectively applied in different perspectives.

Global contrast and brightness as well as sharpness of images were adjusted using Adobe Photoshop (ver. 12.1, Adobe Systems Incorporated, San Jose, CA, USA, RRID:SCR_014199). Stereomicroscopic autofluorescence images were black and white converted in Adobe Photoshop. All figures were assembled with Adobe Illustrator (ver. 15.1, Adobe Systems Incorporated, RRID:SCR_010279).

Data, Materials, and Software Availability. All data needed to evaluate the conclusions in the paper are present in the paper and the *SI Appendix*. All μCT raw datasets can be openly accessed at https://doi.org/10.5281/zenodo.7497684.

ACKNOWLEDGMENTS. We thank all administrative and scientific personnel supporting animal collection at Station Biologique de Roscoff (Sorbonne Université) and Biologische Anstalt Helgoland (Alfred-Wegener-Institut für Polar- und Meeresforschung) for their assistance. We thank Steffen Harzsch for providing laboratory space. We gratefully acknowledge the helpful comments of two anonymous reviewers. Funding: Deutsche Forschungsgemeinschaft grant BR5039/3-1 (G.B.). Assemble Plus grant as part of the European Union's Horizon 2020 research and innovation program under grant agreement no. 730984 (G.B.).

1. A. Trembley, *Mémoires, Pour Servir à l'Histoire d'un Genre de Polypes d'Eau Douce, à Bras en Forme de Cornes* (Verbeek, Leiden, 1744).
2. H. Przibram, *Experimentalzoologie, 2 Regeneration (Wieder-Erzeugung)* (Franz Deuticke, Leipzig, 1909).
3. S. Tiozzo, R. R. Copley, Reconsidering regeneration in metazoans: an evo-devo approach. *Front. Ecol. Evol.* **3**, 67 (2015).
4. L. Bideau, P. Kerner, J. Hui, M. Vervoort, E. Gazave, Animal regeneration in the era of transcriptomics. *Cell. Mol. Life Sci.* **78**, 3941–3956 (2021).
5. A. E. Bely, K. G. Nyberg, Evolution of animal regeneration: Re-emergence of a field. *Trends Ecol. Evol.* **25**, 161–170 (2010).
6. E. E. Zattara, "Axial regeneration in segmented animals. A post-embryonic reboot of the segmentation process" in *Cellular Processes in Segmentation*, A. D. Chipman, Ed. (CRC Press, 2020), chap. 10, pp. 256–292.
7. A. E. Bely, Evolutionary loss of animal regeneration: Pattern and process. *Integr. Comp. Biol.* **50**, 515–527 (2010).
8. G. Giribet, G. D. Edgecombe, The phylogeny and evolutionary history of arthropods. *Curr. Biol.* **29**, R592–R602 (2019).
9. A. Minelli, Arthropod segments and segmentation–Lessons from myriapods, and open questions. *Opuscula Zool.* **51**, 7–21 (2020).
10. F. Alwes, C. Enjolras, M. Averof, Live imaging reveals the progenitors and cell dynamics of limb regeneration. *eLife* **5**, e19766 (2016).
11. D. Maruzzo, L. Bonato, C. Brena, G. Fusco, A. Minelli, "Appendage loss and regeneration in arthropods: A comparative view" in *Crustacea and Arthropod Relationships*, S. Koenemann, R. A. Jenner, Eds. (CRC Press, Boca Raton, 2005), pp. 215–245.
12. A. Minelli, *The Development of Animal Form* (Cambridge University Press, Cambridge, 2003).
13. J. Ewer, How the ecdysozoan changed its coat. *PLoS Biol.* **3**, e349 (2005).
14. E. E. Zattara, A. E. Bely, Phylogenetic distribution of regeneration and asexual reproduction in Annelida: Regeneration is ancestral and fission evolves in regenerative clades. *Invertebrate Biol.* **135**, 400–414 (2016).
15. J. Loeb, Bermerkungen über Regeneration. (1. Über die Regeneration des Rumpfes bei Pantopoden. 2. Zur Theorie der Regenerationserscheinungen). *Arch. Entwickl. Mech.* **2**, 250–256 (1895).
16. D. Maruzzo, F. Bortolin, "Arthropod regeneration" in *Arthropod Biology and Evolution. Molecules, Development, Morphology*, A. Minelli, G. Boxshall, G. Fusco, Eds. (Springer-Verlag, Berlin, 2013), pp. 149–169, 10.1007/978-3-662-45798-6_7.
17. J. A. Ballesteros *et al.*, Comprehensive species sampling and sophisticated algorithmic approaches refute the monophyly of Arachnida. *Mol. Biol. Evol.* **39**, msac021 (2022).
18. J. A. Ballesteros *et al.*, Phylogenomic resolution of sea spider diversification through integration of multiple data classes. *Mol. Biol. Evol.* **38**, 686–701 (2021).
19. J. W. Hedgpeth, On the evolutionary significance of the Pycnogonida. *Smithson. Misc. Collect.* **106**, 1–53 (1947).
20. J. A. Dunlop, J. C. Lamsdell, Segmentation and tagmosis in Chelicerata. *Arthropod Struct. Dev.* **46**, 395–418 (2017).
21. F. Arnaud, R. N. Bamber, The biology of Pycnogonida. *Adv. Mar. Biol.* **24**, 1–96 (1987).
22. K. Frankowski, K. Miyazaki, G. Brenneis, A microCT-based atlas of the central nervous system and midgut in sea spiders (Pycnogonida) sheds first light on evolutionary trends at the family level. *Front. Zool.* **19**, 14 (2022).
23. G. Brenneis, "Pycnogonida (Pantopoda)" in *Structure and Evolution of Invertebrate Nervous Systems*, A. Schmidt-Rhaesa, S. Harzsch, G. Purschke, Eds. (Oxford University Press, 2016), chap. 35, pp. 419–427.
24. J. Ortega-Hernández, R. Lerosey-Aubril, S. R. Losso, J. C. Weaver, Neuroanatomy in a middle Cambrian mollisoniid and the ancestral nervous system organization of chelicerates. *Nat. Commun.* **13**, 410 (2022).
25. J. Bergström, W. Stürmer, G. Winter, *Palaeoisopus*, *Palaeopantopus* and *Palaeothea*, pycnogonid arthropods from the Lower Devonian Hunsrück Slate, West Germany. *Paläontol. Z.* **54**, 7–54 (1980).
26. M. Poschmann, J. Dunlop, A new sea spider (Arthropoda: Pycnogonida) with a flagelliform telson from the Lower Devonian Hunsrück Slate, Germany. *Palaeontology* **49**, 983–989 (2006).
27. A. Dohrn, "Die Pantopoden des Golfes von Neapel und der angrenzenden Meeres-Abschnitte" in *Fauna und Flora des Golfes von Neapel und der angrenzenden Meeres-Abschnitte* (Verlag von Wilhelm Engelmann, Leipzig, 1881), pp. 1–252.
28. G. Brenneis, G. Scholtz, The "ventral organs" of Pycnogonida (Arthropoda) are neurogenic niches of late embryonic and post-embryonic nervous system development. *PLoS ONE* **9**, e95435 (2014).
29. G. Brenneis, G. Scholtz, B. Beltz, Comparison of ventral organ development across Pycnogonida (Arthropoda, Chelicerata) provides evidence for a plesiomorphic mode of late neurogenesis in sea spiders and myriapods. *BMC Evol. Biol.* **18**, 47 (2018).
30. W. Schimkewitsch, V. Dogiel, Ueber Regeneration bei Pantopoden. *Bull. Acad. Imp. Sci. St.-Petersbourg 6* **Ser. 7**, 1147–1156 (1913).
31. H. Helfer, E. Schlottke, *Pantopoda, Dr. H. G. Bronns Klassen und Ordnungen des Tierreichs*, Bd. 5, Abt. IV, Buch 2 (Akademische Verlagsgesellschaft m.b.H., Leipzig, 1935), pp. 1–314.
32. N. Alexeeva, Y. Tamberg, Anatomical changes in postembryonic development of *Pycnogonum litorale*. *J. Morphol.* **282**, 329–354 (2021).
33. G. Lotz, D. Bückmann, Die Häutung und die Exuvie von *Pycnogonum litorale* (Ström) (Pantopoda). *Zool. Jahrb. Anat.* **85**, 529–536 (1968).
34. H.-W. Schmidt, Die Beeinflussing der Häutungen von *Pycnogonum litorale* (Ström) durch exogene und endogene Faktoren. *Oecologia* **7**, 249–261 (1971).
35. K. E. Meyer, D. Bückmann, Die Häutungen des Pantopoden *Pycnogonum litorale* (Ström.). *Verh. dtsch. zool. Ges., Zool. Anz., Suppl.* **1962**, 604–609 (1963).
36. T. H. Morgan, Notes on regeneration. *Biol. Bull.* **6**, 159–172 (1904).
37. H. Ohshima, Six-legged pantopod, an extraordinary case of hypomery in arthropods. *Proc. Imperial Acad. Japan* **18**, 257–262 (1942).
38. L. Galli, E. Colasanto, F. Betti, M. Capurro, Pycnogonids (Arthropoda: Pycnogonida) of Portofino, Ligurian Sea (North-Western Mediterranean Sea). *Eur. Zool. J.* **86**, 241–248 (2019).
39. M.E.-L. Bouvier, Quelque mots sur la variabilité du *Pycnogonum littorale*, Ström. *J. Mar. Biol. Assoc. U. K.* **10**, 207–210 (1914).
40. G. Brenneis, G. Scholtz, A postlarval instar of *Phoxichilidium femoratum* (Pycnogonida, Phoxichilidiidae) with an exceptional malformation. *J. Morphol.* **282**, 278–290 (2021).
41. R. Godelmann, Beiträge zur Kenntnis von *Bacillus rossii* Fabr. mit besonderer Berücksichtigung der bei ihm vorkommenden Autotomie und Regeneration einzelner Gliedmaßen. *Arch. Entwickl. Mech.* **12**, 265–301 (1901).
42. F. Megusar, Die Regeneration der Coleopteren. *Arch. Entwickl. Mech.* **25**, 148–234 (1907).
43. A. Kumar, J. P. Brockes, Nerve dependence in tissue, organ, and appendage regeneration. *Trends Neurosci.* **35**, 691–699 (2012).
44. C. Sinigaglia, M. Averof, The multifaceted role of nerves in animal regeneration. *Curr. Opin. Genet. Dev.* **57**, 98–105 (2019).
45. K. M. Wells, K. Kelley, M. Baumel, W. A. Vieira, C. D. McCusker, Neural control of growth and size in the axolotl limb regenerate. *eLife* **10**, e68584 (2021).
46. P. M. Hopkins, S. Das, "Regeneration in crustaceans" in *The Natural History of the Crustacea, Physiology*, E. S. Chang, M. Thiel, Eds. (Oxford University Press, Oxford, 2015), **4**, chap. 6.
47. B. Boilly, Y. Boilly-Marer, A. E. Bely, Regulation of dorso-ventral polarity by the nerve cord during annelid regeneration: A review of experimental evidence. *Regeneration* **4**, 54–68 (2017).
48. R. P. Ribeiro, C. Bleidorn, M. T. Aguado, Regeneration mechanisms in Syllidae (Annelida). *Regeneration* **5**, 26–42 (2018).
49. E. C. Seaver, D. M. de Jong, Regeneration in the segmented annelid *Capitella teleta*. *Genes* **12**, 1769 (2021).
50. A. Planques, J. Malem, J. Parapar, M. Vervoort, E. Gazave, Morphological, cellular and molecular characterization of posterior regeneration in the marine annelid *Platynereis dumerilii*. *Dev. Biol.* **445**, 189–210 (2019).
51. E.-L. Bouvier, Observations sur les Pycnogonomorphes et principalement sur le *Pentapycnon Geayi*, espèce tropical á dix pattes. *C. R. Hebd. Seances Acad. Sci.* **152**, 491–494 (1911).
52. W. G. Fry, J. W. Hedgpeth, The fauna of the Ross Sea. Part 7. Pycnogonida 1: Colossendeidae, Pycnogonidae, Endeidae, Ammotheidae. *N. Z. Dept. Sci. Ind. Res. Bull.* **198**, 1–139 (1969).
53. D. J. Siveter, M. D. Sutton, D. E. G. Briggs, D. J. Siveter, A silurian sea spider. *Nature* **431**, 978–980 (2004).
54. G. Brenneis, E. V. Bogomolova, C. P. Arango, F. Krapp, From egg to "no-body": An overview and revision of developmental pathways in the ancient arthropod lineage Pycnogonida. *Front. Zool.* **14**, 6 (2017).
55. D. Waloszek, A. Maas, The evolutionary history of crustacean segmentation: A fossil-based perspective. *Evol. Dev.* **7**, 515–527 (2005).
56. Y. Liu *et al.*, Three-dimensionally preserved minute larva of a great-appendage arthropod from the early Cambrian Chengjiang biota. *Proc. Natl. Acad. Sci. U.S.A.* **113**, 5542–5546 (2016).
57. A. G. Lai, A. A. Aboobaker, EvoRegen in animals: Time to uncover deep conservation or convergence of adult stem cell evolution and regenerative processes. *Dev. Biol.* **433**, 118–131 (2018).
58. A. S. Alvarado, Regeneration in the metazoans: Why does it happen? *BioEssays* **22**, 578–590 (2000).
59. G. Scholtz, "Segmentation. A zoological concept of seriality" in *Cellular Processes in Segmentation*, A. D. Chipman, Ed. (CRC Press, Boca Raton, 2020), chap. 1, pp. 3–25.
60. K. H. Tomaschko, E. Wilhelm, D. Bückmann, Growth and reproduction of *Pycnogonum litorale* (Pycnogonida) under laboratory conditions. *Mar. Biol.* **129**, 595–600 (1997).
61. K. Vilpoux, D. Waloszek, Larval development and morphogenesis of the sea spider *Pycnogonum litorale* (Ström, 1762) and the tagmosis of the body of Pantopoda. *Arthropod Struct. Dev.* **32**, 349–383 (2003).
62. G. Scholtz, G. Brenneis, The pattern of a specimen of *Pycnogonum litorale* (Arthropoda, Pycnogonida) with a supernumerary leg can be explained with the "boundary model" of appendage formation. *Sci. Nat.* **103**, 13 (2016).
63. J. W. Hammond, D. Cai, K. J. Verhey, Tubulin modifications and their cellular functions. *Curr. Opin. Cell Biol.* **20**, 71–76 (2008).